Farnesyl transferase inhibitors impair chromosomal maintenance in cell lines and human tumors by compromising CENP-E and CENP-F function

Katherine Schafer-Hales,[1] Jon Iaconelli,[1] James P. Snyder,[2] Andrew Prussia,[2] James H. Nettles,[2] Adel El-Naggar,[4] Fadlo R. Khuri,[1] Paraskevi Giannakakou,[3] and Adam I. Marcus[1]

[1]Winship Cancer Institute, [2]Department of Chemistry, Emory University, Atlanta, Georgia; [3]Weill Medical College, Cornell University, New York, New York; and [4]M. D. Anderson Cancer Center, Houston, Texas

Abstract

Farnesyl transferase inhibitors (FTI) exhibit anticancer activity as a single agent in preclinical studies and show promise in combination with other therapeutics in clinical trials. Previous studies show that FTIs arrest cancer cells in mitosis; however, the mechanism by which this occurs is unclear. Here, we observed that treatment of various cancer cell lines with the FTI lonafarnib caused mitotic chromosomal alignment defects, leaving cells in a pseudometaphase state, whereby both aligned chromosomes and chromosomes juxtaposed to the spindle poles (termed ''lagging chromosomes'') were observed in the same cell. To determine how this occurs, we investigated the functionality of two farnesylated mitotic proteins, CENP-E and CENP-F, which mediate chromosomal capture and alignment. The data show that lonafarnib in proliferating cancer cells depletes CENP-E and CENP-F from metaphase but not prometaphase kinetochores. Loss of CENP-E and CENP-F metaphase localization triggered aberrant chromosomal maintenance, causing aligned chromosomes to be prematurely released from the spindle equator and become lagging chromosomes, resulting in a mitotic delay. Furthermore, lonafarnib treatment reduces sister kinetochore tension and activates the BubR1 spindle checkpoint, suggesting that farnesylation of CENP-E and CENP-F is critical for their functionality in maintaining kinetochore-microtubule interactions. Importantly, apparently similar chromosomal alignment defects were observed in head and neck tumors samples from a phase I trial with lonafarnib, providing support that lonafarnib disrupts chromosomal maintenance in human cancers. Lastly, to examine how farnesylation could regulate CENP-E in mediating kinetochore-microtubule attachments, we examined possible docking motifs of a farnesyl group on the outer surface of the microtubule. This analysis revealed three hydrophobic patches on the tubulin dimer for insertion of a farnesyl group, alluding to the possibility of an association between a farnesyl group and the microtubule. [Mol Cancer Ther 2007;6(4):1317–28]

Introduction

It is estimated that ~60 eukaryotic proteins, including small GTPases, co-chaperones, membrane-associated proteins, and mitotic proteins (1) are post-translationally modified by the addition of a farnesyl group. This enzymatic process, catalyzed by farnesyl transferase (FT), is targeted by a family of anticancer agents known as the FT inhibitors (FTI). FTIs show potent cytotoxicity as a single agent in preclinical studies (2–4) and have shown clinical promise in combination with other therapeutic strategies (5–7). However, the molecular mechanism leading to cell death after FT inhibition remains unclear. Originally, the most provocative candidates were the ras oncogenes, which are farnesylated before insertion into the plasma membrane and are mutated in a variety of cancers (8), but a link between FTI efficacy and ras mutational status has not been established (9–11). Therefore, research efforts have focused on dissecting the molecular consequences of FT inhibition in cancer cells.

One early observation was that FTI treatment results in G_2-M arrest, such that cells accumulate in mitosis and display a monopolar microtubule spindle with a ring of chromosomes (12, 13). This phenotype lends itself to the possibility that FTIs disrupt the functionality of a farnesylated mitotic protein(s), resulting in aberrant spindle formation and chromosomal translocation. Interestingly, there are only two known farnesylated mitotic proteins, CENP-E and CENP-F (also known as mitosin), both of which are found on the centromere alongside microtubules and specifically localize to the outer kinetochore plate during prophase. In particular, CENP-E is required for efficient capture and attachment of spindle microtubules by the kinetochore (14) and acts as a signal-transducing linker responsible for silencing BubR1-dependent mitotic checkpoint signaling (15). Gene silencing of CENP-E leads to chromosome mis-segregation and mitotic delay (16), as well as unstable kinetochore-microtubule capture and

Received 11/14/06; revised 2/7/07; accepted 2/22/07.

Grant support: NIH/National Cancer Institute Lung Cancer Program Project grant 1PO1 CA116676 (F.R. Khuri, P. Giannakakou, and A.I.Marcus) and NIH grant CA-69571 (J.P. Snyder).

The costs of publication of this article were defrayed in part by the payment of page charges. This article must therefore be hereby marked *advertisement* in accordance with 18 U.S.C. Section 1734 solely to indicate this fact.

Note: K. Schafer-Hales and J. Iaconelli contributed equally to this work.

Requests for reprints: Adam I. Marcus, Winship Cancer Institute, Emory University, Atlanta, GA 30322. Phone: 404-778-4597. E-mail: adam.marcus@emory.org

doi:10.1158/1535-7163.MCT-06-0703

chromosomal instability (17). The role of CENP-F has been more enigmatic, but recent data show that CENP-F mediates kinetochore-microtubule attachments, and farnesylation of CENP-F is required for both G_2-M progression (18) and microtubule capture (19).

Because CENP-E and CENP-F are farnesylated mitotic proteins and FTI treatment results in mitotic arrest, the question as to whether FTIs can block the farnesylation of CENP-E and CENP-F was previously investigated. The results show that the FTI, lonafarnib (SCH66336), inhibits their farnesylation *in vitro*, but surprisingly does not disrupt their localization to the kinetochore in prometaphase arrested cancer cells (12, 20). However, a more recent study in nocodazole-arrested cells showed that FTI treatment depletes CENP-F at the kinetochore and along the nuclear envelope (18). In view of this ambiguity, further analysis of the effects of FTIs on the functionality of CENP-E and CENP-F would prove useful to determine if FTIs do indeed affect CENP-E and CENP-F function in proliferating cancer cells and, if so, what role this plays in the anticancer properties of FTIs.

In the present work, we analyze the impact of FTI treatment on chromosomal positioning during mitosis to investigate how lonafarnib causes aberrant mitosis. We observe for the first time that lonafarnib treatment results in mislocalized chromosomes during metaphase, whereby one or more chromosomes are found at the microtubule spindle poles. To investigate the molecular basis of this defect, we show that lonafarnib treatment depletes CENP-E and CENP-F from metaphase kinetochores of proliferating cancer cells and causes aberrant chromosomal maintenance at the spindle equator. These cells display a significantly reduced sister kinetochore tension and have an activated BubR1 spindle checkpoint, suggesting that farnesylation of CENP-E and CENP-F is critical for their functionality in maintaining chromosomal alignment during metaphase. Importantly, apparently similar chromosomal alignment defects were observed in head and neck tumors samples from a phase I trial, with lonafarnib providing support that lonafarnib disrupts chromosomal maintenance in human cancers. By combining this data with computational analysis of a putative farnesyl group/microtubule interaction, we propose a model whereby the farnesyl group can dock into three putative hydrophobic patches on the tubulin dimer and strengthen the link between the kinetochore and microtubule during mitosis.

Materials and Methods

Cell Culture

Cell lines were maintained in RPMI 1640 supplemented with 5% FCS, non–essential amino acids, and 0.1% penicillin/streptomycin. All lines were cultured at 37°C in a humidified atmosphere with 5% CO_2.

Reagents

Lonafarnib (SCH66336) was provided by Schering Plough Research Institute (Kenilworth, NJ). FTI-277 was purchased from EMD Biosciences, Inc. (San Diego, CA). Both FTIs were dissolved in DMSO at a concentration of 10 mmol/L, and aliquots were stored at −20°C. Stock solutions were diluted to the desired final concentrations with growth medium just before use. Taxol was obtained from Calbiochem (San Diego, CA), aliquoted to 1 or 10 μmol/L in DMSO and stored at 4°C.

Immunofluorescence Analysis

Immunofluorescence was done as previously described (21). The following primary antibodies were used: α-tubulin at 1:1,000 (Chemicon International; Temecula, CA), CENP-E at 1 μg/mL (Immuquest, Ingleby, Barwick, United Kingdom), CENP-F at 1:100 (BD Biosciences, San Jose, CA), and BubR1 at 1:500 (Rockland Immunochemicals, Philadelphia, PA), with an incubation time of 1 h for tubulin (room temperature) and overnight at 4°C for CENP-E, CENP-F, and BubR1. For kinetochore staining, an anti-ACA antibody (Antibodies Incorporated, Davis, CA) was used at 1:250, with a overnight incubation at 4°C. The secondary antibodies all were goat Alexa-conjugated antibodies (488, 555, and 648) against the appropriate species and used at 1:500 for 1 h at room temperature (Invitrogen, Carlsbad, CA). Fixed cells were imaged using a Zeiss LSM 510 (Zeiss, Thornwood, NY) confocal microscope with either a 63× (numerical aperture, 1.4) or 100× (numerical aperture, 1.4) Apochromat objective. To stain DNA for mitotic cell counting, Sytox Green (Molecular Probes, Eugene, OR) or 4′,6-diamidino-2-phenylindole was added to the Gel Mount mounting media (Biomeda Corp., Foster City, CA) according to manufacturer's protocol.

Cell Growth Assay

The sulforhodamine B (SRB) cytotoxicity assays were adapted from Skehan et al. (22) and done as previously described (23). For statistical analysis, a correlation coefficient was determined using the two arrays of data (i.e., IC_{50} and percentage of mitotic cells with lagging chromosomes).

Live-Cell Confocal Imaging

Either A549 or 1A9 cells were transfected with a H2B:GFP plasmid (PharMingen, San Jose, CA) using LipofectAMINE 2000 (Invitrogen) according to the manufacturer's protocol. Cells were plated on live-cell imaging chambers (Mattek, Ashland, MA) and allowed to adhere overnight. Cells were then imaged directly or treated with lonafarnib for 16 h using a Perkin-Elmer (Norwalk, CT) Ultraview ERS spinning disc confocal as described previously (23). Images were acquired using either a 63× or 100× objective, and multiple optical slices were acquired either every minute or every 5 s. Once acquired, images were exported in TIF format and imported into Metamorph 6.1 (Universal Imaging, Downingtown, PA), where images were thresholded, and the mean pixel intensity was calculated for the various fluorophores (e.g., CENP-F, BubR1).

Image Analysis of Kinetochore Distances and Chromosome Tracking

Immunofluorescence was done as described above. Images of kinetochores (anti-ACA), tubulin, and DNA were exported in TIF format to Metamorph 6.1, and measurements of kinetochore distances were done as described previously (24). Only kinetochores in the same

focal plane were measured. At least 50 kinetochore pairs for each experimental group were measured. Chromosomes were tracked using the ''track points'' feature on Metamorph. The origin was determined to be the initial location of the chromosome before it exiting from the metaphase plate.

Analysis of Human Head and Neck Cancer Samples

A phase Ib trial was conducted with lonafarnib in patients with squamous cell carcinoma of the head and neck scheduled for surgery (25, 26). Patients were randomized to one of three b.i.d. dose levels (100, 200, or 300 mg) or no treatment. The oral agent lonafarnib was administered for 8 to 14 days in the immediate preoperative period. Baseline tumor biopsies and the surgical specimens were obtained for analysis. A total of 35 patients entered the trial, and 27 received lonafarnib. Paraffin-embedded sections of matched pre– and post–lonafarnib-treated head and neck tumor samples were obtained for only four patients due to limited sample supply. Sections were stained with H&E to assess mitotic DNA. Approximately 100 mitotic cells were counted in each experimental group. Images of the tumor cells were acquired using a Zeiss Axioplan microscope with either 40× or 100× Plan-Apo oil immersion objectives.

Computational Analysis of the Farnesyl Group/Tubulin Interaction

The microtubule model used in this study was built in Sybyl 7.0 using the geometric template of a 13 protofilament microtubule solved by cryoelectron microscopy (EM) at 8 Å resolution (27). This template orients protofilament tetramers from the atomic resolution model of αβ-tubulin dimers 1JFF (28), to best correlate with the microtubule map. The final alignment of our model was checked for placements of helices and sheets within the EM map consistent with the original work. No additional modeling was done; therefore, this model lacks the NH_2-terminal H1-S2 loop and alpha M-loop, as does 1JFF. Although specific interactions at the lateral interface differ between the two systems, the close fit of the taxol-bound M-loop from Zn-induced sheets to the density of the microtubule suggests high geometric similarity between the two systems.

A truncated model of farnesylated CENP-E (Fig. 7A, *structure 1*) was constructed in Maestro (Schrodinger, Inc., New York, NY) using an acetyl group attached to the terminal cysteine as a placeholder for the rest of the CENP-E protein. The structure was docked using GLIDE (29) into several hydrophobic sites on the 1JFF αβ-tubulin model

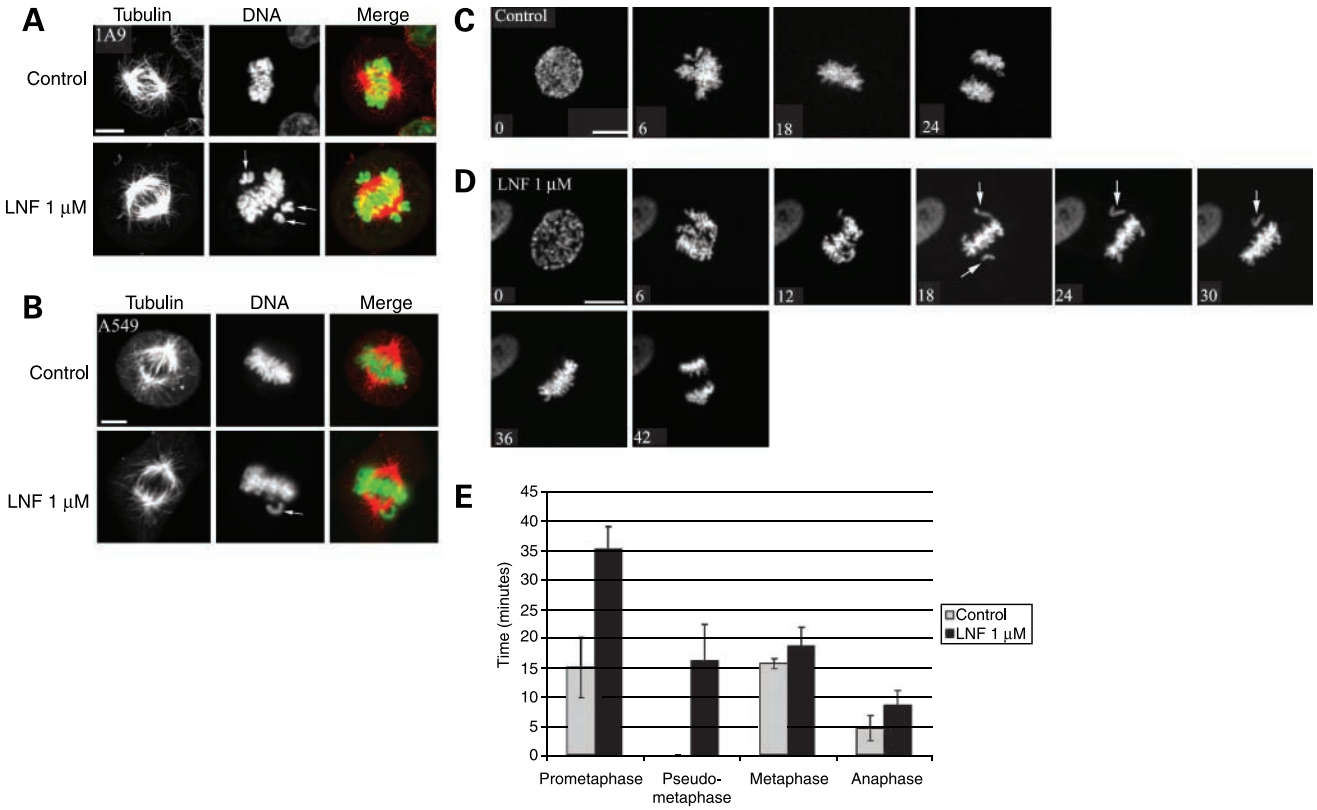

Figure 1. Lonafarnib treatment causes lagging chromosomes at the mitotic spindle poles. **A** and **B,** immunofluorescence images of 1A9 ovarian carcinoma cells (**A**) and A549 lung carcinoma cells (**B**) either untreated or treated with lonafarnib. *Arrows,* lagging chromosomes. **C** and **D,** A549 cells transfected with H2B:GFP were imaged using confocal microscopy. Representative time frames of control (**C**) and lonafarnib-treated (**D**) cells are shown. *Bar,* 10 μm. **E,** temporal analysis of lonafarnib-treated and untreated cells during the various stages of mitosis. Pseudometaphase is defined as the presence of both lagging chromosomes and aligned chromosomes. *Bars,* SD.

(28), in which hydrogens were added using GLIDE's protein preparation protocol. The largest possible grids at each site (14 Å > movement box from the midpoint of the ligand) were used for docking to generate a diverse pool of 50 poses at each docking site. The best poses were selected based on good hydrophobic contact, a favorable conformation of the farnesyl group, and an orientation of the acetyl placeholder in a manner that would allow the rest of the CENP-E to avoid clashing with either the αβ-dimer itself, or with adjacent αβ-dimers of the microtubule. The best poses were relaxed using short, low-temperature molecular dynamics in Sybyl (Sybyl 7.0 Tripos Inc., St. Louis, MI). Molecular dynamics solves Newton's laws of motion to simulate the effect of thermal energy and motion on a molecular system, allowing us to relax the farnesyl group in the protein. Molecular dynamics was carried out with following characteristics: fixed protein residues >4 Å surrounding the ligand, Tripos force field, Kollman all-atom atomic charges on protein, Pullman atomic charges on ligand, dielectric constant 4.5, NTV ensemble, 300 to 500 fs, 20 K, 0.5 fs time step. Molecular dynamics treatment was followed by minimization until convergence (Powell method, other parameters similar to molecular dynamics). Measurements on the microtubule structure were done with our reconstruction of the model built by Downing et al. (28) using cryoelectron microscopy.

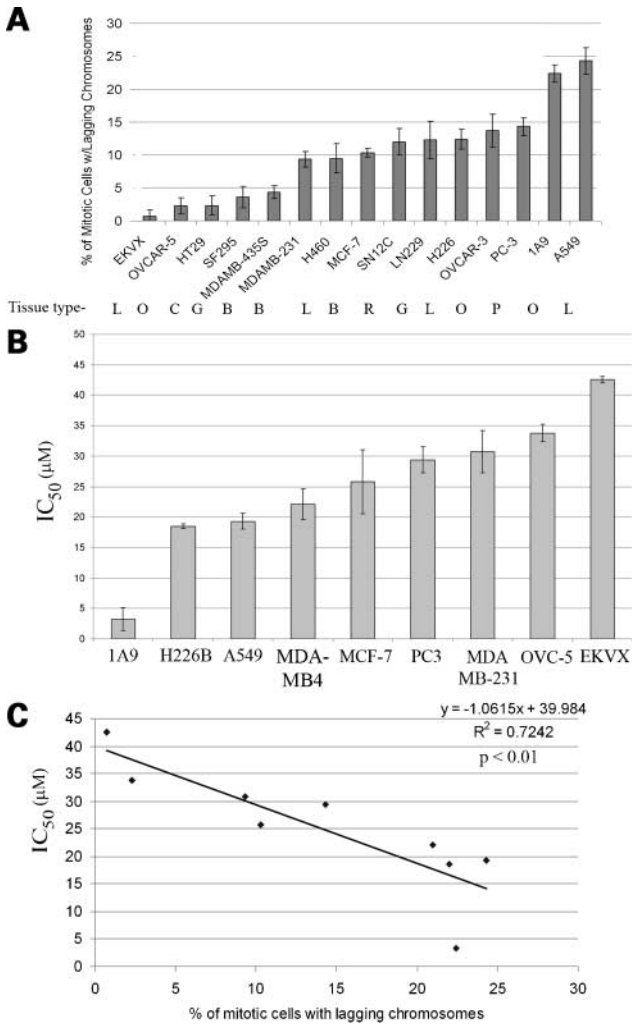

Figure 2. The extent of lagging chromosomes correlates with lonafarnib antiproliferative efficacy. **A,** graph showing the percentage of mitotic cells with lagging chromosomes in 15 human cancer cell lines. *L,* lung; *O,* ovarian; *C,* colon; *G,* glioblastoma; *B,* breast; *R,* renal. **B,** graph showing lonafarnib IC_{50} values for nine different human cancer cell lines. **C,** IC_{50} of nine human cancer cell lines plotted as a function of the percentage of mitotic cells having lagging chromosomes.

Results

Lonafarnib Treatment Induces Lagging Chromosomes in Human Cancer Cells

To observe the effects of FTIs on mitosis, microtubule spindle formation and chromosome localization were assessed in 1A9 ovarian cancer cells. Untreated control cells in metaphase exhibited a bipolar microtubule spindle with chromosomes tightly aligned along the spindle equator. After 16 h treatment with lonafarnib (1 μmol/L), the metaphase microtubule spindle remained morphologically normal (Fig. 1A), and there were no changes in spindle depth or width (Supplementary Fig. S1).[5] Analysis of chromosomal localization, however, revealed that 22% of metaphase cells had both aligned and spindle pole–associated chromosomes in the same cell resulting in a pseudometaphase state (Fig. 1A). These spindle pole–associated chromosomes, termed lagging chromosomes, were also observed in A549 lung cancer cell lines (Fig. 1B) as well as in other cell lines tested (Supplementary Fig. S1). Similarly, treatment of 1A9 and A549 cells with the commercially available FTI, FTI-277, also resulted in lagging chromosomes (data not shown), indicating that this aberrant phenotype is not specific to lonafarnib, but instead occurs with all FTIs tested.

To further examine chromosomal positioning, live-cell confocal imaging was employed using A549 cells transiently transfected with an H2B:GFP construct. Cells were first imaged when chromosomes began to condense (prophase) and were monitored until the completion of cytokinesis. In untreated cells (n = 10), chromosomes on average were aligned 12 min after condensation, and anaphase occurred at 24 min (Fig. 1C). In contrast, cells treated with 1 μmol/L lonafarnib for 16 h (n = 10) did not show fully aligned chromosomes until 36 min, and lagging chromosomes were, on average, observed at 18 min (Fig. 1D; Movie S1).[5] These lagging chromosomes eventually did insert into the metaphase plate at 36 min; anaphase then occurred at 42 min. Quantitative temporal analysis shows that lonafarnib-treated cells spend an additional 20 min in prometaphase, of which 15 min are in pseudometaphase, defined as the presence of both lagging chromosomes and fully aligned chromosomes (Fig. 1E). Interestingly, similar analysis of 1A9

[5] Supplementary material for this article are available at Molecular Cancer Therapeutics Online (http://mct.aacrjournal.org/).

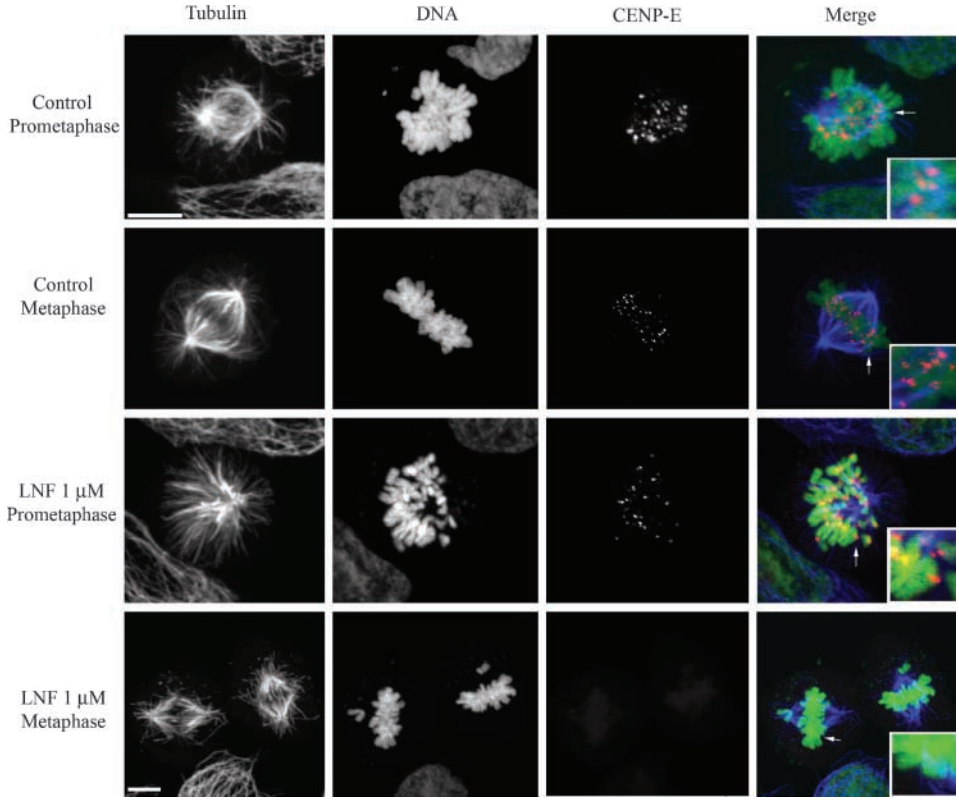

Figure 3. Lonafarnib depletes CENP-E from the kinetochore during metaphase but not prometaphase. Immunofluorescence staining of tubulin, DNA, and CENP-E in untreated and lonafarnib-treated cells. Representative mitotic cells in prometaphase and metaphase are shown for control and lonafarnib-treated cells. *Insets,* magnified images of the area designated by arrow. *Bar,* 10 μm.

cells transfected with H2B:GFP show similar lagging chromosomes; however, in most cases, after the completion of cell division, multiple nuclei would form from a single daughter nucleus. (Supplementary Fig. S1; Movie S2).[5]

Lastly, previous reports show that the combination of lonafarnib with paclitaxel results in a synergistic increase in acetylated tubulin, likely due to HDAC6 inhibition (21, 30). However, here, lonafarnib was used as a single agent, and consistent with previous findings, we did not observe significant effects on acetylated tubulin levels (Supplementary Fig. S1D),[5] but as expected, we did have inhibition of farnesylation of HDJ-2, a FT client protein (Supplementary Fig. S1E).[5]

Prevalence of Lagging Chromosomes Correlates with Lonafarnib Antiproliferative Efficacy in Human Cancer Cell Lines

To determine if the presence of lagging chromosomes plays a significant role in the antiproliferative mechanism of action of lonafarnib, we correlated the presence of lagging chromosomes with the IC_{50} of lonafarnib in a variety of human cancer cell lines from different tissue types. To do this, the percentage of mitotic cells in 15 human cancer cell lines displaying lagging chromosomes after 1 μmol/L lonafarnib treatment (16 h) was recorded based on immunofluorescence analysis of DNA and tubulin. This result showed that the presence of lagging chromosomes in cell lines was variable. For example, certain cell lines such as 1A9 and A549 exhibited 20% to 25% of mitotic cells with lagging chromosomes, whereas EKVX, SKVMEL, and OVC-5 evidenced <5% (Fig. 2A). In conjunction, cell growth assays with lonafarnib were done in cell lines chosen to represent low (EKVX, OVC-5, MDA-MB-231), medium (MCF-7, MDA-MB4, PC3), and high (1A9, H226B, A549) populations of mitotic cells displaying lagging chromosomes. These data show that the IC_{50} values among the cell lines were also variable ranging from 9 to 45 μmol/L (Fig. 2B). Importantly, when the IC_{50} for each cell line was plotted against the percentage of mitotic cells with lagging chromosomes, a significant negative correlation was observed ($R^2 = -0.72$; $P < 0.01$; Fig. 2C). That is, the presence of lagging chromosomes is associated with a low lonafarnib IC_{50}, whereas the absence of lagging chromosomes correlates with a high IC_{50}. In addition, we did not observe any correlation with cell doubling time (data not shown). This analysis therefore suggests that the effect of lonafarnib on chromosomal alignment plays an important role in lonafarnib's antiproliferative efficacy.

Lonafarnib Treatment Depletes CENP-E and CENP-F from Metaphase Kinetochores

Previous reports have shown that FTI treatment does not alter CENP-E and CENP-F kinetochore localization during prometaphase in cancer cells (20); however, our observation shows a novel defect, such that lonafarnib treatment causes a pseudometaphase state due to defective chromosomal alignment and maintenance. Moreover, other groups have shown that depletion of CENP-E and CENP-F results in similar lagging chromosomes, and we have confirmed this finding (Supplementary Fig. S2A).[5]

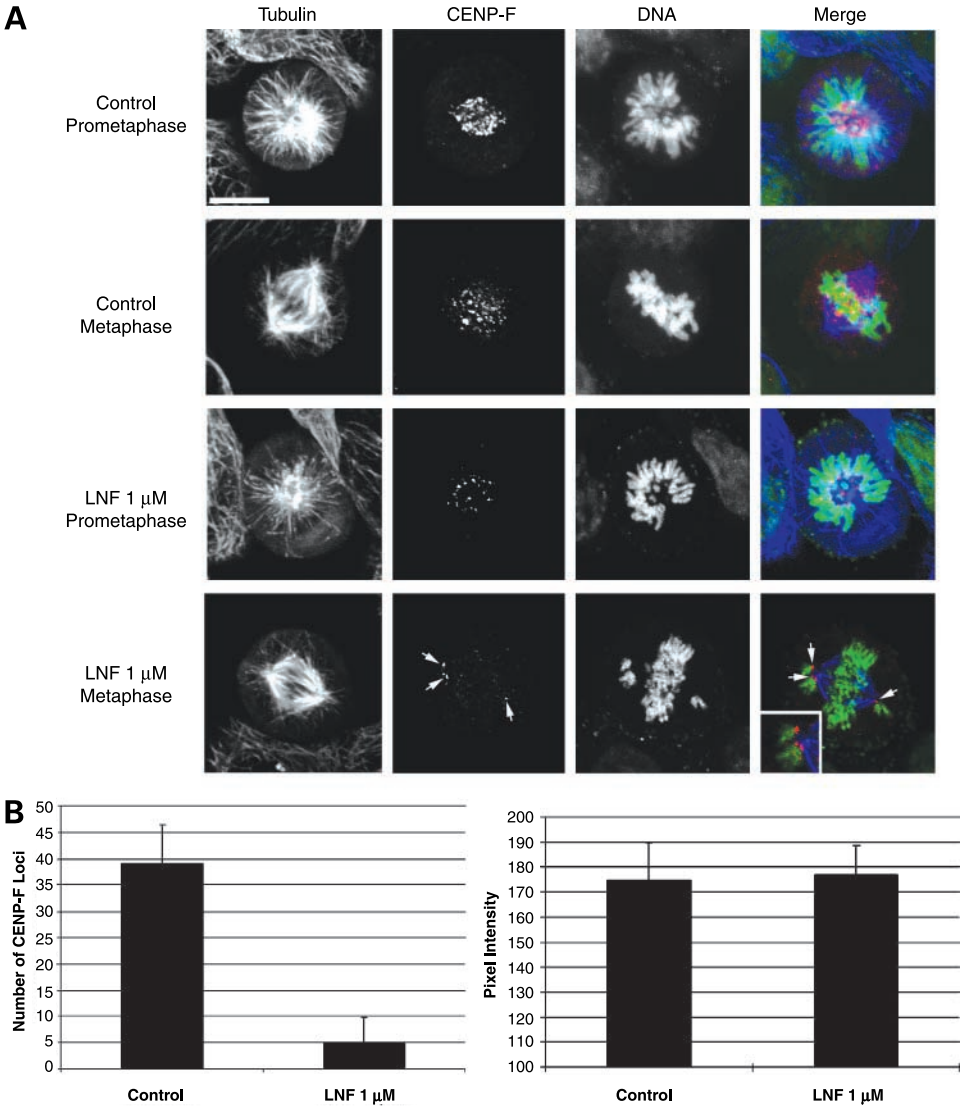

Figure 4. Lonafarnib depletes CENP-F from the kinetochore during metaphase except on lagging chromosomes. **A,** immunofluorescence staining of tubulin, DNA, and CENP-F in untreated and lonafarnib-treated cells. Representative mitotic cells in prometaphase and metaphase are shown for control and lonafarnib-treated cells. *Insets,* magnified images of the area designated by arrow. *Bar,* 10 μm. **B,** graph showing image quantification of the number of CENP-F loci and pixel intensity of the CENP-F signal. *Bars,* SD.

We therefore postulated that their functionality may be compromised in metaphase and not prometaphase; thus, we evaluated the effects of lonafarnib on CENP-E and CENP-F localization during different stages of mitosis. Immunofluorescence images of tubulin, DNA, and CENP-E in untreated prometaphase 1A9 cells show an immature spindle (i.e., lacking two distinct spindle poles) and dispersed chromosomes, and CENP-E is present on the kinetochore (Fig. 3). As mitosis progresses, untreated metaphase cells develop a bipolar spindle with chromosomes aligned along the spindle equator, and CENP-E always remains localized to the chromosomes at the kinetochores (Fig. 3). In lonafarnib-treated prometaphase cells, spindles also displayed a normal architecture, dispersed chromosomes, and CENP-E was indeed localized to the kinetochore similar to control cells (Fig. 3). However, in lonafarnib-treated pseudometaphase cells, CENP-E staining was completely absent at the kinetochores, both in aligned and lagging chromosomes (Fig. 3). This was observed in nearly all pseudometaphase mitotic cells analyzed as well as metaphase cells that lacked lagging chromosomes, indicating that CENP-E metaphase localization may be farnesylation dependent.

Similar analysis of CENP-F was done, and an analogous pattern was observed. Upon lonafarnib treatment, CENP-F was still present on kinetochores in prometaphase, but was absent from kinetochores during metaphase (Fig. 4A). Strikingly, however, CENP-F still remained on the kinetochore of lagging chromosomes, which differed from that of CENP-E, because it was absent on all chromosomes. Further quantitative analysis shows that the number of CENP-F loci on metaphase chromosomes per cell significantly decreases after lonafarnib treatment ($P < 0.05$), but the mean signal intensity of CENP-F at the lagging chromosomes remains the same (Fig. 4B), indicating that CENP-F binding affinity for lagging chromosomes was not

affected. Overall, these results show that like CENP-E, CENP-F is depleted from metaphase kinetochore after lonafarnib treatment; however, CENP-F still remains on lagging chromosomes with similar intensity as untreated cells.

Lonafarnib Disrupts Chromosomal Maintenance at the Spindle Equator

During mitosis, chromosomes must be first translocated to the spindle equator, then maintained at this site for anaphase to proceed correctly. We show that lonafarnib depletes the centromeric proteins CENP-E and CENP-F from metaphase kinetochores, both of which maintain kinetochore-microtubule interactions at the spindle equator. Therefore, we wanted to determine how lonafarnib treatment and, consequently, CENP-E and CENP-F depletion alter chromosomal maintenance at the spindle equator. To assess this, chromosomal movements were assessed in live A549 cells transfected with H2B:GFP (n = 10 cells) and treated with 1 μmol/L lonafarnib for 8 h. High spatiotemporal optical sections were acquired to observe chromosomal movements at the spindle equator. Strikingly, in cells treated with lonafarnib, we observed individual chromosomes that were already aligned, slowly exiting the spindle equator and drifting toward the spindle poles to become lagging chromosomes. This created a mitotic delay, and ultimately, the chromosome was recaptured by the spindle and realigned (Fig. 5A; Movie S4). Representative time frames (a total of n = 15 chromosomes in 12 cells were observed) show that in this case, the aligned chromosome (arrow) exits the spindle equator and slowly drifts outward toward the spindle poles for from 30 to 108 s, pauses, and then is rapidly realigned from 153 to 177 s. Further quantitative analysis of all 15 chromosomes reveals that the chromosomal exit velocity was 1.8 μm/min, whereas the reentry velocity was much more rapid, with a mean 6.2 μm/min (Fig. 5B and C). This suggests that chromosomes passively diffused away from the spindle equator but were actively recruited back, presumably recaptured by another microtubule.

Lonafarnib Activates the BubR1 Spindle Checkpoint and Weakens Kinetochore Tension

CENP-E has been shown to be the signal transducing linker responsible for silencing BubR1-dependent mitotic checkpoint signaling by capturing the kinetochores of spindle microtubules (15, 31). Because we show that CENP-E localization is compromised in the presence of lonafarnib, we predict that BubR1 will remain activated in lonafarnib-treated cells. To test this, we examined the expression and localization of BubR1 in control and lonafarnib-treated cells. In control metaphase cells, aligned chromosomes show minimal BubR1 kinetochore staining (Fig. 6A), indicating that chromosomes are effectively aligned and poised to segregate. Not surprisingly, in lonafarnib-treated cells, the lagging chromosome displays intense BubR1 staining, indicating that the checkpoint is active due to a failure to align correctly (Fig. 6A). Interestingly, however, in the presence of lonafarnib, the majority of apparently aligned chromosomes also had an activated BubR1 spindle checkpoint at the kinetochore (Fig. 6A). Quantitative analysis revealed that even after only 8 h of lonafarnib treatment (1 μmol/L), a significant increase of BubR1 signal intensity was observed (Fig. 6B). Based on this observation, it seems that although the majority of chromosomes seem aligned in the presence of lonafarnib, significant defects remain that are severe enough to activate the BubR1 spindle checkpoint.

To explore these defects, we examined kinetochore tension of both aligned and lagging chromosomes in

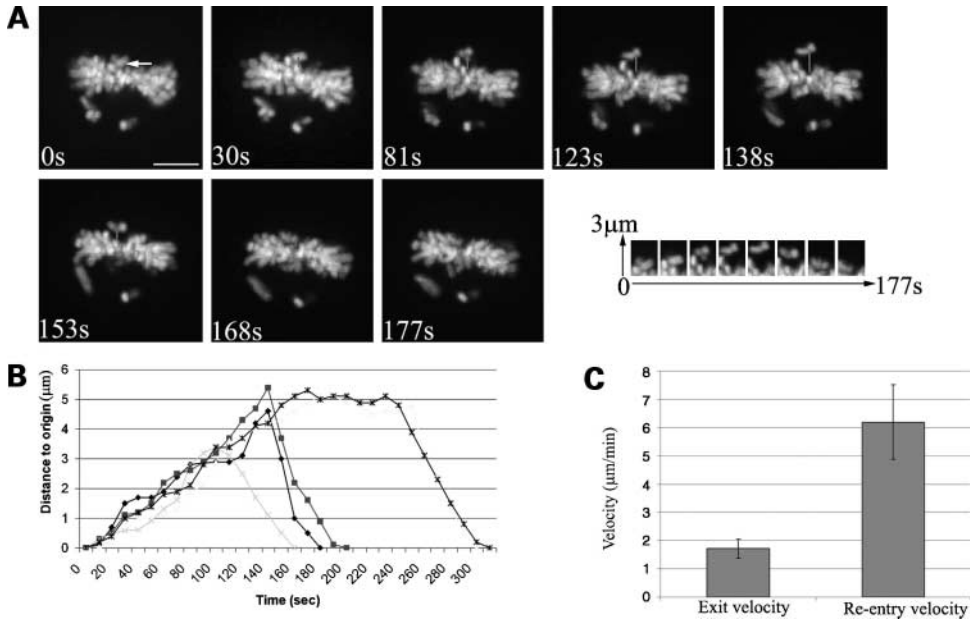

Figure 5. Lonafarnib impairs chromosomal maintenance at the spindle equator. A549 cells were transfected with H2B:GFP and imaged using live-cell confocal microscopy. **A,** live-cell imaging after 8 h treatment of lonafarnib (1 μmol/L). Images show a chromosome (*arrow*) exiting the metaphase plate at 30 s and reentering at 138 s. *Bar,* 5 μm. White line shows how chromosomal distances from the spindle equator were measured. **B,** plot of five representative chromosomes that were tracked when exiting and reentering the metaphase plate. Distances were measured relative to the initial location of the chromosomes on the metaphase plate. **C,** graph plotting the exit and reentry velocity of n = 10 chromosomes. *Bars,* SD. All times are in seconds.

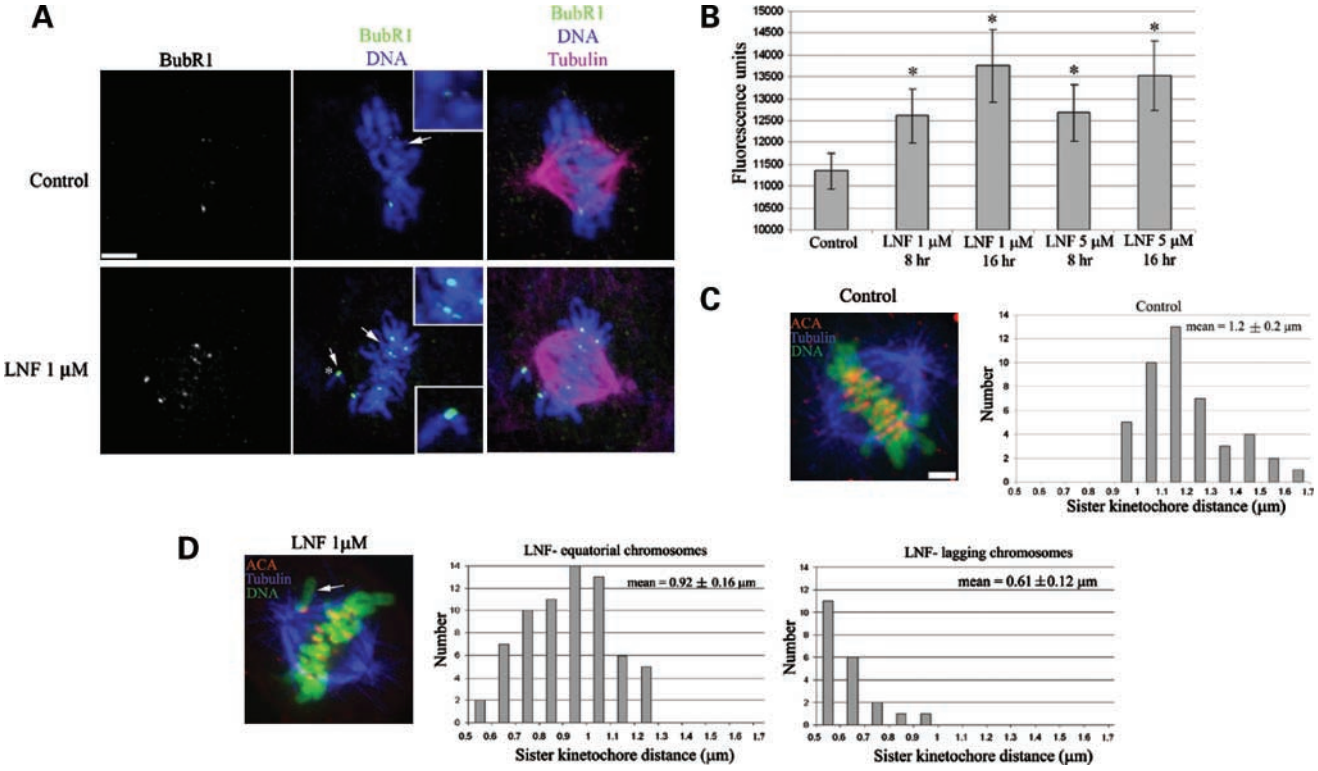

Figure 6. Lonafarnib activates the BubR1 spindle checkpoint and reduces sister kinetochore tension. **A,** immunofluorescence staining of BubR1, tubulin, and DNA in A549 cells treated with lonafarnib for 16 h. Control metaphase cells have relatively low levels of BubR1 staining. Lonafarnib treatment results induces BubR1 staining on lagging chromosomes (*asterisk*) and aligned chromosomes relative to control. *Arrows,* region shown in the inset. *Bar,* 10 μm. **B,** graph displaying BubR1 fluorescence intensity with various drug treatments. *, *P* value <0.05 compared with control. **C** and **D,** histograms (*right*) showing the distances between kinetochores of sister chromatids were determined based on immunofluorescence staining (*left*) of tubulin, DNA, and ACA in control and lonafarnib-treated cells. *Arrow,* lagging chromosomes. *Bars,* 2 μm.

lonafarnib-treated cells. Kinetochore tension generated by an infiltrating microtubule is required for mitosis to proceed (32), and a single unattached kinetochore can delay anaphase onset (33). If lonafarnib treatment activates the spindle checkpoint resulting in defective chromosomal maintenance, we would expect to observe reduced kinetochore tension after lonafarnib treatment compared with control cells. To test this, we did immunofluorescence staining of kinetochores, tubulin, and DNA after lonafarnib treatment at 1 μmol/L for 16 h. The interkinetochore distance, which serves as a reliable indicator of tension across the kinetochore pair (34, 35), was measured in both equatorial and lagging chromosomes with an anticentromere antibody (ACA; see Materials and Methods). Kinetochore distances in control A549 cells were, on average, 1.2 ± 0.2 μm (Fig. 6C). Upon treatment of these cells with lonafarnib, the mean sister kinetochore distance was reduced to 0.92 ± 0.16 μm (Fig. 6D). Furthermore, in cases where the sister kinetochores of lagging chromosomes could be discerned, the sister kinetochore distance was reduced even further to 0.61 ± 0.12 μm (Fig. 6D). Based on these results, we conclude that lonafarnib treatment reduces sister kinetochore tension in equatorial and, to a greater extent, lagging chromosomes, suggesting that lonafarnib treatment may weaken kinetochore-microtubule interactions leading to inefficient chromosomal maintenance.

Potential Farnesyl Group Interaction Sites on Microtubules

Both CENP-E and CENP-F mediate kinetochore microtubule attachments and are farnesylated at a CAAX motif at the COOH terminus. Our analysis shows that they are both depleted from metaphase kinetochores after lonafarnib treatment, indicating that farnesylation regulates their localization. In an attempt to provide a rudimentary model of how a farnesyl group could mediate the association of CENP-E with microtubules, we have examined possible docking motifs for structure 1 (Fig. 7A) on the outer surface of microtubules. This structure was selected because it corresponds to the modified COOH terminus of proteins with a CAAX box following sequential prenylation by farnesyl PPi at cysteine, proteolytic removal of AAX, and COOH-terminal carboxyl methylation (36). We presume that the CENP-E interacts with the outside of the tubular structure. Examination of the αβ-tubulin dimer in the context of the 8-Å resolution model of the microtubule structure (27) suggests that the hydrophobic surface of the protein dimer between adjacent protofilaments at the

αβ-interface, as well as the surface near helices H9 and H10 of the α subunit, are likely regions of temporary association between CENP-E and microtubules mediated by the farnesyl group. Figure 7B depicts the external surface of the αβ-tubulin dimer within the microtubule in terms of hydrophobic (*brown-green*) and hydrophilic (*blue*) character. It is evident that a number of hydrophobic patches characterized by depressions in the surface of the dimer might serve as binding sites for the farnesyl tail of structure 1.

To test this, we employed the GLIDE docking protocol (29, 37) in an attempt to locate suitable candidate binding pockets for structure 1, a surrogate for farnesylated CENP-E in which the unknown tertiary structure has been replaced by an acetyl group. The program operates by first performing an on-the-fly conformational analysis of the molecule to be docked. Suitable conformations are then translated and rotated in three-dimensional to find a structural match for a user-selected portion of the protein surface. GLIDE docking of structure 1 was applied with two provisions. First, as mentioned above, only hydrophobic candidate pockets on the outer surface of microtubules that are not occluded by adjacent protofilaments were examined. Second, docking poses of structure 1 that directed the cysteine α-carbon and the adjacent NH and acetyl groups into the surface of the tubulin subunits were rejected. Only those poses that orient the modified cysteine outward compatible with attachment to the COOH terminus of the CENP-E protein were accepted. This exercise provided three plausible docking poses represented by three separate sites. The initial poses were refined by low-temperature molecular dynamics followed by structure optimization (Fig. 7C).

Sites A and B are both located at the αβ interface, roughly opposite the GDP binding site (both sites are ~23 Å from GDP). Site A is in a pocket formed by residues of β-H12, a loop between β-H8 and β-B7, and the α residues of loop between H11 and H12. Near site A, site B is in a pocket formed by residues of β-H10, the loop between β-H10 and β-B9, and the α residues of H11. In site C, however, the structure docks at roughly the midpoint of the α subunit, ~25 Å from site B and 45 Å from site A, in a hydrophobic pocket formed by two α loop regions: H9 to B8, and H10 to B9. In microtubules, site C is just 10 Å from the residues of an adjacent α subunit. In all three sites, the acetyl group capping the cysteine residue is positioned so that the rest of the CENP-E protein would not clash with the microtubule structure.

For the docking poses to be chemically reasonable, they should be in energetically favorable conformations. One basis for comparison is the degree of similarity of docked conformations of the farnesyl group with those found in X-ray crystal structures. Figure 7D shows the similarity of the predicted docking poses to the experimentally derived conformations of the farnesyl groups in the crystal structure of undecaprenyl PPi synthase (PDB code 1V7U;

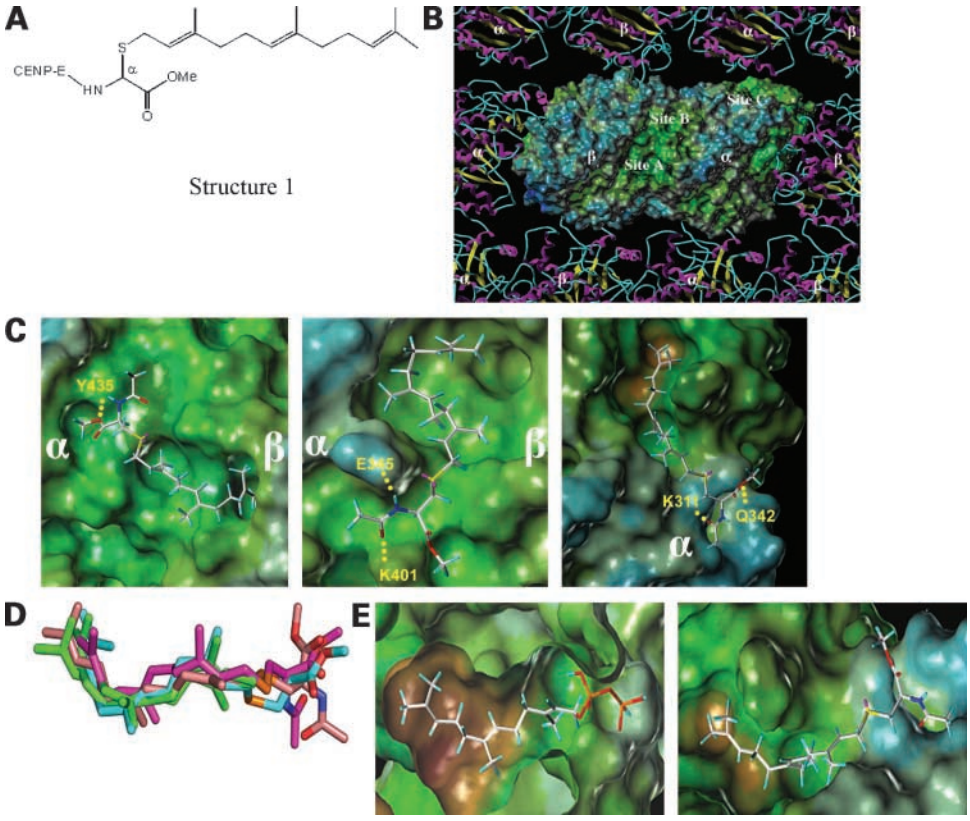

Figure 7. The tubulin dimer possesses three potential sites for interaction with a farnesyl group. **A,** structure 1 used in the analysis. **B,** Connolly surface of the αβ-tubulin dimer colored by hydrophobicity (*brown-green,* hydrophobic; *blue,* hydrophilic); the surrounding microtubule structure is shown as α-helices, β-sheets, and loops. Three sites were found that are suitable for farnesyl docking. **C,** docking results for structure 1 in sites A, B, and C. Sites A and B are at the αβ interface of the tubulin dimer. Site C is on the α subunit, near the point of lateral interaction with an adjacent α subunit. **D,** docking poses of structure 1 (*cyan,* site A; *magenta,* site B; and *pink,* site C) superimposed onto the two farnesyl groups found in the X-ray crystal structure 1V7U (green carbons). **E,** hydrophobicity-mapped Connolly surfaces for the farnesyl group binding cavity found in the X-ray structure 1V7U (*left*) and a predicted farnesyl binding cavity on tubulin (*right*).

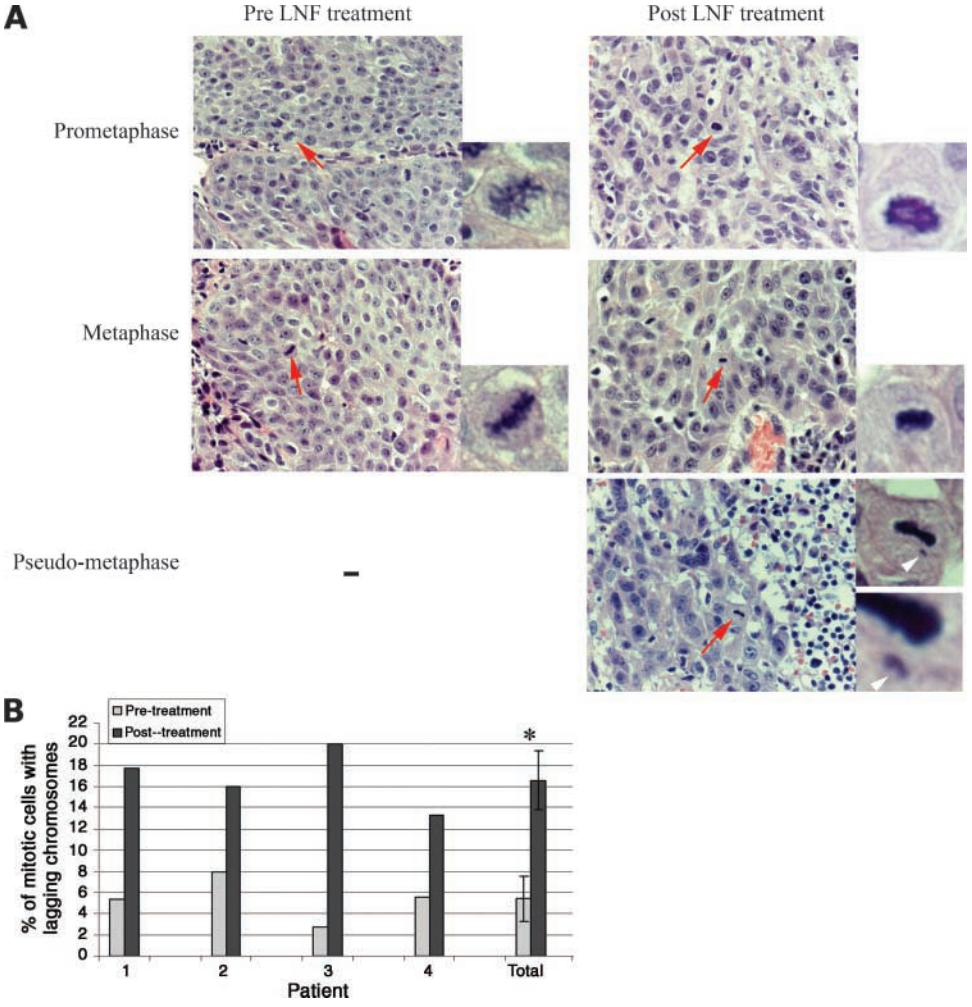

Figure 8. Lonafarnib causes lagging chromosomes in human head and neck tumors. **A,** H&E staining of pre– and post–lonafarnib-treated tumors from head and neck cancer patients. Images are representative examples of prometaphase, metaphase, and pseudometaphase mitotic cells. *Insets*, a magnified image of the cell indicated with the arrow. **B,** quantitative analysis of the percentage of mitotic cells with lagging chromosomes in four paired patient samples.

ref. 38). The same overall shape of the farnesyl group in both the predicted poses and the experimental structures suggests that the poses are indeed in biologically relevant conformations. The farnesyl group binds proteins at highly hydrophobic sites, as seen in the binding cavity in the X-ray crystal structure (Fig. 7E, *left*). Predicted farnesyl binding sites (Fig. 7E, *right*) are also hydrophobic, but to a lesser degree than those found in the crystal structures.

Lonafarnib Treatment Is Associated with Lagging Chromosomes in Head and Neck Cancer Patients

Because we show that lonafarnib treatment disrupts CENP-E and CENP-F localization leading to defective chromosomal alignment and maintenance, we next wanted to determine if this aberrant mitosis is observed in clinical samples. To do this, paraffin-embedded sections of pre– and post–lonafarnib-treated human head and neck tumors were obtained from a phase I clinical trial. The paired specimens of four patients were stained with H&E, and the presence of lagging chromosomes in mitotic cells was surveyed. Representative images of prometaphase, metaphase, and pseudometaphase are shown for pre- and posttreatment samples (Fig. 8A, with additional examples in Supplementary Fig. S2C).[5] Each showed lagging chromosomes that appeared similar to those observed in the cell lines. Interestingly, when the total number of mitotic tumor cells among all patients containing lagging chromosomes was compared in pre- and posttreatment samples, there was a significant increase from 5% to 20% ($P < 0.05$) of mitotic cells having lagging chromosomes in these two groups, respectively. Furthermore, using paired pre- and posttreatment samples from each individual patient, lonafarnib treatment caused a drastic increase in the number of mitotic cells containing lagging chromosomes in each patient (Fig. 8B). Thus, this evidence provides strong support that lonafarnib disrupts chromosomal maintenance in head and neck human tumors.

Discussion

Lonafarnib Impairs Chromosomal Maintenance by Depleting CENP-E and CENP-F from Metaphase Kinetochores

When FTIs were shown to induce a G_2-M arrest in cancer cell lines, it was hypothesized that their antimitotic

properties were due to inhibition of CENP-E and CENP-F farnesylation (12, 20). Initial experiments addressing this question were ambiguous because lonafarnib only affected the *in vitro* association of CENP-E with microtubules but did not affect CENP-E or CENP-F kinetochore localization in arrested cells (12), although more recently, Hussein and Taylor (18) showed that CENP-F farnesylation is required for G2-M progression, CENP-F degradation, and CENP-F kinetochore localization in nocodazole-arrested cells. Our data in proliferating cancer cells is consistent with these results by demonstrating that CENP-E and CENP-F prometaphase kinetochore localization is indeed unaffected by lonafarnib treatment; however, the present data additionally show that both CENP-E and CENP-F are depleted from metaphase kinetochores in rapidly dividing cancer cells at physiologically relevant doses of lonafarnib (Figs. 3 and 4). Interestingly, CENP-F remains on the lagging chromosomes, indicating that it may serve as a cellular sensing mechanism for chromosomal misalignment. Taken together, we conclude that inhibition of CENP-E and CENP-F farnesylation by lonafarnib alters their metaphase localization and suggests that their metaphase functionality is farnesylation dependent, whereas during prometaphase, their localization remains intact, suggesting that prometaphase functionality is farnesylation independent.

In addition, we believe that loss of CENP-E and CENP-F activity results in the observed lagging chromosomes because similar lagging chromosomes are observed when CENP-E or CENP-F is depleted by small interfering RNA Supplementary Fig. S2A and B,[5] antibody microinjection, or gene excision (14, 16, 17). Moreover, we show that inhibition of farnesylation by lonafarnib causes defective chromosomal maintenance at the spindle equator (Fig. 5A–C), activates the BubR1 spindle checkpoint (Fig. 6A and B), and reduces sister kinetochore tension (Fig. 6C and D). Importantly, CENP-E has been shown to be the signal-transducing linker responsible for silencing BubR1-dependent mitotic checkpoint signaling by capturing the kinetochores of spindle microtubules (15, 31). Because CENP-E and CENP-F are proposed to mediate kinetochore capture and stability by microtubules (14, 19, 39, 40), we propose that lonafarnib induced loss of CENP-E and CENP-F, activates BubR1 checkpoint, and leads to weak kinetochore-microtubule interactions, resulting in aberrant chromosomal maintenance and lagging chromosomes.

It is also important to note that lonafarnib treatment causes mitotic delay and not mitotic arrest, suggesting that inhibition of CENP-E and CENP-F localization only partially inhibits function, or that redundant mechanisms rescue defects in CENP-E and/or CENP-F, allowing mitosis to proceed. We tend to believe the latter because CENP-E and CENP-F localization on the kinetochore is undetectable after lonafarnib treatment, suggesting that protein function during this time period was completely disrupted. Furthermore, it has been shown that chromosome alignment can be achieved via redundant mechanisms even if CENP-E function is compromised (39), perhaps suggesting that in this case, defective chromosomal maintenance by lonafarnib is rescued by an alternative, farnesylation-independent mechanism.

Because it has been previously shown that CENP-E stabilizes kinetochore-microtubule interactions and that the *in vitro* association of CENP-E with microtubules is farnesylation dependent (20), we hypothesized that the CENP-E farnesyl group interacts with microtubules to maintain chromosomes at the spindle equator. In an attempt to provide a rudimentary model illustrating how a farnesyl moiety might mediate the association of CENP-E with microtubules, possible docking motifs on the outer surface of the microtubule were examined. Using structure 1 (Fig. 7A) as a surrogate for the farnesylated COOH terminus of CENP-E resulted in the identification of three potential hydrophobic patches on the tubulin dimer and a compatible fit of the farnesyl tail to them. Although the results are preliminary, they may provide insight into how a farnesyl group could be essential in regulating the association of CENP-E with the microtubule. In fact, previous reports show that CENP-E microtubule binding *in vitro* is farnesylation dependent (20), suggesting that the COOH-terminal farnesyl group of CENP-E may play an important role in maintaining the CENP-E/microtubule association. Moreover, both CENP-E and CENP-F are capable of binding microtubules at their COOH termini (40, 41) in addition to their NH_2-terminal microtubule binding domain, which is where the farnesylation CAAX motif is located. One possibility is that CENP-E binds microtubules with its NH_2-terminal motor domain and uses the COOH-terminal farnesylation group to cross-link microtubules at the spindle equator; however, additional *in vitro* experiments are necessary to test this hypothesis.

Clinical Relevance of Lonafarnib-Induced Lagging Chromosomes

All FTIs tested were capable of inducing lagging chromosomes in a panel of 15 cell lines (examples shown in Supplementary Fig. S1), suggesting that this is a global mechanism of action shared by this class of agents. We observed, however, that the percentage of mitotic cells with lagging chromosomes among the cell lines varies, and statistical analysis shows that lonafarnib IC_{50} and the presence of lagging chromosomes were negatively correlated (Fig. 2). Specifically, lines having a high percentage of cells with lagging chromosomes show more sensitivity to lonafarnib than lines with a low percentage of lagging chromosomes. This significant association between chromosomal alignment defects and cell growth inhibition suggests that the two are related, and therefore, chromosomal alignment defects may play a significant role in lonafarnib's antiproliferative mechanism. Importantly, these effects may not just be limited to cell lines because our results from a phase I clinical trial show that lonafarnib significantly increases the number of head and neck tumor cells with lagging chromosomes among all pre- and posttreatment samples ($P < 0.05$; Fig. 8). These lagging

chromosomes seem nearly identical to those observed in cell lines, and the number of cells with lagging chromosomes in all four paired pre- and posttreatment samples more than tripled after lonafarnib treatment. We could not determine if the presence of lagging chromosomes correlates with response to treatment because the number of paired patient samples was limited; nevertheless, this finding provides clinical support to our observations and suggests that lonafarnib could also disrupt chromosomal maintenance in human tumor cells.

Acknowledgments

We thank Kenneth Downing of the Lawrence Berkeley National Laboratory for providing the microtubule template coordinates used in this study. This work is dedicated to the memory of Dr. Robert Apkarian of Emory University.

References

1. Reid TS, Terry KL, Casey PJ, Beese LS. Crystallographic analysis of CaaX prenyltransferases complexed with substrates defines rules of protein substrate selectivity. J Mol Biol 2004;343:417 – 33.

2. Smalley KS, Eisen TG. Farnesyl transferase inhibitor SCH66336 is cytostatic, pro-apoptotic and enhances chemosensitivity to cisplatin in melanoma cells. Int J Cancer 2003;105:165 – 75.

3. Sun J, Blaskovich MA, Knowles D, et al. Antitumor efficacy of a novel class of non-thiol – containing peptidomimetic inhibitors of farnesyltransferase and geranylgeranyltransferase I: combination therapy with the cytotoxic agents cisplatin, Taxol, and gemcitabine. Cancer Res 1999;59:4919 – 26.

4. Haluska P, Dy GK, Adjei AA. Farnesyl transferase inhibitors as anticancer agents. Eur J Cancer 2002;38:1685 – 700.

5. Khuri FR, Glisson BS, Kim ES, et al. Phase I study of the farnesyltransferase inhibitor lonafarnib with paclitaxel in solid tumors. Clin Cancer Res 2004; 10:2968 – 76.

6. Kim ES, Kies MS, Fossella FV, et al. Phase II study of the farnesyltransferase inhibitor lonafarnib with paclitaxel in patients with taxane-refractory/ resistant nonsmall cell lung carcinoma. Cancer 2005;104:561 – 9.

7. David E, Sun SY, Waller EK, et al. The combination of the farnesyl transferase inhibitor lonafarnib and the proteasome inhibitor bortezomib induces synergistic apoptosis in human myeloma cells that is associated with down-regulation of p-AKT. Blood 2005;106:4322 – 9.

8. Barbacid M. ras genes. Annu Rev Biochem 1987;56:779 – 827.

9. End DW, Smets G, Todd AV, et al. Characterization of the antitumor effects of the selective farnesyl protein transferase inhibitor R115777 *in vivo* and *in vitro*. Cancer Res 2001;61:131 – 7.

10. Nagasu T, Yoshimatsu K, Rowell C, Lewis MD, Garcia AM. Inhibition of human tumor xenograft growth by treatment with the farnesyl transferase inhibitor B956. Cancer Res 1995;55:5310 – 4.

11. Sepp-Lorenzino L, Ma Z, Rands E, et al. A peptidomimetic inhibitor of farnesyl:protein transferase blocks the anchorage-dependent and -independent growth of human tumor cell lines. Cancer Res 1995;55: 5302 – 9.

12. Crespo NC, Ohkanda J, Yen TJ, Hamilton AD, Sebti SM. The farnesyltransferase inhibitor, FTI-2153, blocks bipolar spindle formation and chromosome alignment and causes prometaphase accumulation during mitosis of human lung cancer cells. J Biol Chem 2001;276:16161 – 7.

13. Moasser MM, Sepp-Lorenzino L, Kohl NE, et al. Farnesyl transferase inhibitors cause enhanced mitotic sensitivity to taxol and epothilones. Proc Natl Acad Sci U S A 1998;95:1369 – 74.

14. Schaar BT, Chan GK, Maddox P, Salmon ED, Yen TJ. CENP-E function at kinetochores is essential for chromosome alignment. J Cell Biol 1997; 139:1373 – 82.

15. Mao Y, Desai A, Cleveland DW. Microtubule capture by CENP-E silences BubR1-dependent mitotic checkpoint signaling. J Cell Biol 2005; 170:873 – 80.

16. Tanudji M, Shoemaker J, L'Italien L, et al. Gene silencing of CENP-E by small interfering RNA in HeLa cells leads to missegregation of chromosomes after a mitotic delay. Mol Biol Cell 2004;15:3771 – 81.

17. Putkey FR, Cramer T, Morphew MK, et al. Unstable kinetochore-microtubule capture and chromosomal instability following deletion of CENP-E. Dev Cell 2002;3:351 – 65.

18. Hussein D, Taylor SS. Farnesylation of Cenp-F is required for G_2/M progression and degradation after mitosis. J Cell Sci 2002;115:3403 – 14.

19. Bomont P, Maddox P, Shah JV, Desai AB, Cleveland DW. Unstable microtubule capture at kinetochores depleted of the centromere-associated protein CENP-F. EMBO J 2005;24:3927 – 39.

20. Ashar HR, James L, Gray K, et al. Farnesyl transferase inhibitors block the farnesylation of CENP-E and CENP-F and alter the association of CENP-E with the microtubules. J Biol Chem 2000;275:30451 – 7.

21. Marcus AI, Zhou J, O'Brate A, et al. The synergistic combination of the farnesyl transferase inhibitor lonafarnib and paclitaxel enhances tubulin acetylation and requires a functional tubulin deacetylase. Cancer Res 2005;65:3883 – 93.

22. Skehan P, Storeng R, Scudiero D, et al. New colorimetric cytotoxicity assay for anticancer-drug screening. J Natl Cancer Inst 1990;82:1107 – 12.

23. Marcus AI, Peters U, Thomas SL, et al. Mitotic kinesin inhibitors induce mitotic arrest and cell death in Taxol-resistant and -sensitive cancer cells. J Biol Chem 2005;280:11569 – 77.

24. Zhou J, Panda D, Landen JW, Wilson L, Joshi HC. Minor alteration of microtubule dynamics causes loss of tension across kinetochore pairs and activates the spindle checkpoint. J Biol Chem 2002;277:17200 – 8.

25. Kies M, Clayman GL, El-Naggar AK, et al. Induction therapy with SCH 66336: A farnesyl transferase inhibitor in squamous cell carcinoma (SCC) of the head and neck [abstract 896]. In: Proc Am Soc Clin Oncol 2001;20.

26. Hassan KWW, Wang L, Lee H-Y, et al. Dephosphorlyation and down-regulation of AKT is associated with Farnesyltransferase inhibitor (SCH66336) treatment in head and neck squamous cell carcinoma cell lines [abstract]. In: Proc Am Assoc Cancer Res 2002.

27. Li H, DeRosier DJ, Nicholson WV, Nogales E, Downing KH. Microtubule structure at 8 A resolution. Structure 2002;10:1317 – 28.

28. Lowe J, Li H, Downing KH, Nogales E. Refined structure of α β-tubulin at 3.5 A resolution. J Mol Biol 2001;313:1045 – 57.

29. Friesner RA, Banks JL, Murphy RB, et al. Glide: a new approach for rapid, accurate docking and scoring. 1. Method and assessment of docking accuracy. J Med Chem 2004;47:1739 – 49.

30. Marcus AI, O'Brate AM, Buey RM, et al. Farnesyltransferase inhibitors reverse taxane resistance. Cancer Res 2006;66:8838 – 46.

31. Yao X, Abrieu A, Zheng Y, Sullivan KF, Cleveland DW. CENP-E forms a link between attachment of spindle microtubules to kinetochores and the mitotic checkpoint. Nat Cell Biol 2000;2:484 – 91.

32. Nicklas RB, Waters JC, Salmon ED, Ward SC. Checkpoint signals in grasshopper meiosis are sensitive to microtubule attachment, but tension is still essential. J Cell Sci 2001;114:4173 – 83.

33. Rieder CL, Schultz A, Cole R, Sluder G. Anaphase onset in vertebrate somatic cells is controlled by a checkpoint that monitors sister kinetochore attachment to the spindle. J Cell Biol 1994;127:1301 – 10.

34. Waters JC, Chen RH, Murray AW, Salmon ED. Localization of Mad2 to kinetochores depends on microtubule attachment, not tension. J Cell Biol 1998;141:1181 – 91.

35. Mitchison T, Evans L, Schulze E, Kirschner M. Sites of microtubule assembly and disassembly in the mitotic spindle. Cell 1986;45:515 – 27.

36. Zubay GL. Biochemistry. 4th ed. Dubuque (IA): Wm. C. Brown Publishers; 1998. p. xxxi, 540, [64].

37. Halgren TA, Murphy RB, Friesner RA, et al. Glide: a new approach for rapid, accurate docking and scoring. 2. Enrichment factors in database screening. J Med Chem 2004;47:1750 – 9.

38. Chang SY, Ko TP, Chen AP, Wang AH, Liang PH. Substrate binding mode and reaction mechanism of undecaprenyl pyrophosphate synthase deduced from crystallographic studies. Protein Sci 2004;13:971 – 8.

39. McEwen BF, Chan GK, Zubrowski B, et al. CENP-E is essential for reliable bioriented spindle attachment, but chromosome alignment can be achieved via redundant mechanisms in mammalian cells. Mol Biol Cell 2001;12:2776 – 89.

40. Feng J, Huang H, Yen TJ. CENP-F is a novel microtubule-binding protein that is essential for kinetochore attachments and affects the duration of the mitotic checkpoint delay. Chromosoma 2006;115:320 – 9.

41. Liao H, Li G, Yen TJ. Mitotic regulation of microtubule cross-linking activity of CENP-E kinetochore protein. Science 1994;265:394 – 8.